Int. J. Heat Mass Transfer. Vol. 33, No. 5, pp. 771–783, 1990
Printed in Great Britain

0017–9310/90 $3.00+0.00
Pergamon Press plc

Thermal processes during the interaction of optical radiation pulses with heterogeneous laminated biotissues

V. K. PUSTOVALOV and I. A. KHORUNZHII
The Byelorussian Polytechnic Institute, Minsk, 220027, U.S.S.R.

(*Received* 23 *May* 1988)

Abstract—Energy absorption, heat transfer and thermochemical processes occurring during the interaction of optical radiation pulses with pigmented spherical and spheroidal granules in heterogeneous laminated biotissues are investigated theoretically. A system of equations is formulated which describes interaction processes for short radiation pulses of length $t_p < 10^{-6}$ s and for long radiation pulses of length $t_p > 10^{-6}$ s. Numerical solutions of this system give the space–time temperature distributions, degrees of thermochemical transformations of the biotissue molecules around the pigmented granules and in the volume of laminated biotissues. The possibility for selective interaction between short radiation pulses and pigmented biotissues is shown which results in the formation of thermodenaturation microregions inside and near the pigmented granules.

1. INTRODUCTION

INVESTIGATION of the interaction of optical radiation with heterogeneous laminated biotissue is of particular interest for photobiology and photomedicine and also for working out safety norms to handle intense optical radiation sources [1–3]. This attaches a great importance to studies on numerical simulation of the processes of radiation interaction with biotissues aimed at clarifying the role of different mechanisms in the interaction and investigating the effects of radiation and medium parameters on the result of interaction. Of special interest is the interaction of optical radiation pulses with the biotissues of the eyeground as the organ most vulnerable to damage by radiation. Moreover, the photocoagulation of the eye tissue has been found successful in ophthalmology [4]. Theoretical investigations of the thermal action of optical radiation on the laminated tissues of the eyeground were conducted in refs. [5–9] with consideration for the difference between optical and thermophysical parameters of various layers. The tissues within each layer were assumed to be homogeneous. This allowed a satisfactory agreement between experimental and theoretical results for radiation pulses of length $t_p > 10^{-4}$ s. At the same time, the results of theoretical and experimental investigations for shorter pulses of length $t_p \leqslant 10^{-4}$ s diverge significantly and this divergence cannot be explained within the framework of the models of refs. [5–9]. It was noted earlier [2, 10–13] that the basic factor responsible for this divergence is the nonuniformity (heterogeneity) of the separate layers of the eyeground tissue. In particular, in the pigmented epithelium layer (PE) the bulk of radiation energy (up to 90%) is absorbed by melanoprotein granules (MPGs) of spherical and spheroidal shape and small sizes of about 0.5–1 μm. According to the authors of refs. [10, 11], the heat transfer (thermal relaxation) characteristic time comprises $t_1 \sim 10^{-6}$ s. When $t_p \leqslant t_1$, the radiation energy absorbed by the granules does not succeed in being transferred to the surrounding medium and when irradiated the granules are heated up severely. When $t_p > t_1$, the granules absorb radiation energy and exchange heat with the surrounding medium intensively, thus ensuring its uniform heating. In refs. [10, 11] an attempt was made to consider the heating of a single granule by a short radiation pulse, but these were appraising studies which only indicated the importance and necessity of taking into account the granular structure of pigmented biotissue layers.

It follows from the aforegoing that it was of great interest to undertake theoretical investigation of radiation propagation, energy absorption, heat transfer and thermochemical processes during the interaction of optical radiation pulses with the pigmented biotissue layers with regard for their granular structure. Such a study was made in the present work. The interaction of short ($t_p < 10^{-6}$ s) and long ($t_p < 10^{-6}$ s) radiation pulses with spherical and spheroidal granules is considered with regard for the non-linear thermal conductivity of the medium and thermochemical processes. Based on numerical simulation, space–time distributions of the process parameters are obtained.

2. MATHEMATICAL FORMULATION OF THE PROBLEM

Consider the propagation of a beam of optical radiation with wavelength λ and with a certain dis-

NOMENCLATURE

A	complex amplitude of electromagnetic field electric vector
C	heat capacity of medium substance
C_0	heat capacity of granule substance
D_b	characteristic diameter of radiation beam
D_0	diaphragm diameter
E_0	energy density of radiation pulse
F	focal distance of optical system
f	degree of thermochemical transformations of biotissue molecules
ΔH	difference of enthalpies of initial and activated states
h	Planck constant
I	radiation intensity
I_0	initial radiation intensity on beam axis
j_h	density of energy flux removed by heat conduction
k	wave vector
k_B	Boltzmann constant
K_{ab}	efficiency factor for absorption of radiation by a granule
K_{sc}	efficiency factor for scattering of radiation by a granule
N_0	concentration of granules
Q	power density of energy generation
R	radial coordinate of cylindrical coordinate system
R_b	characteristic radius of radiation beam
R_g	universal gas constant
R_0	diaphragm radius
r	radial coordinate with origin at granule centre
r_a	small semiaxis of spheroidal granule
r_b	large semiaxis of spheroidal granule
r_0	radius of spherical granule
S_0	surface area of granule
ΔS	difference of entropies of initial and activated states
T	temperature
T_m	temperature of medium
T_0	temperature of granule
T_∞	initial temperature
t	time
t_p	pulse length
t_l	characteristic time of heat transfer of granule
V_0	volume of granule
x	coordinate of radiation propagation
x_i	boundary of the ith layer.

Greek symbols

α	coefficient of radiation attenuation
α_{ab}	coefficient of radiation absorption
α_{sc}	coefficient of radiation scattering
λ	length of radiation wave
κ	thermal conductivity
ξ	spheroidal coordinate
ρ	density of medium substance
ρ_0	density of granule substance
Φ	Fresnel number
χ	thermal diffusivity of medium.

Subscripts

ab	absorption
c	cell
d	denaturation
g	gas
i	number of layer
m	medium
max	maximum
n	normalized
p	pulse
sc	scattering
t	threshold
∞	initial value.

tribution of radiation intensity I over the section in a laminated medium along the x-axis. The radiation beam axis coincides with the x-axis of the cylindrical coordinate system x, R which, together with the scheme of the eyeground layers [9], is represented in Fig. 1. Individual layers have different optical and thermophysical properties, their parameters having been taken from refs. [5, 8, 9]. The interfaces between the layers x_i ($i = 0, 1, 2, \ldots$) are perpendicular to the x-axis, the thickness of the ith layer equals $\Delta x_i = x_i - x_{i-1}$, for example, $x_3 - x_2 = 5$ μm, $x_4 - x_3 = 20$ μm, $x_5 - x_4 = 80$ μm [9]. Let the PE layer with the boundaries x_2 and x_3 and thickness $x_3 - x_2$ contain an ordered system of spherical and spheroidal granules with the characteristic size of about 0.5–1 μm which absorbs and scatters the radiation energy, and the remaining layers be homogeneous. For simplicity the granules are assumed to be monodispersed. The radiation propagation in the laminated medium is described by the quasi-stationary equation of transfer

$$\frac{\partial I}{\partial x} + (\alpha_{abi} + \alpha_{sci})I = 0 \qquad (1)$$

in which in the case of a heterogeneous layer containing granules $\alpha_{ab3} = N_0 S_s K_{ab}$, $\alpha_{ab3} = N_0 S_s K_{sc}$, where $S_s = \pi r_0^2$ is for a sphere

$$S_s = \pi r_a^2 r_b \left[r_b^2 \sin^2\left(\frac{\pi}{2} - \beta\right) + r_a^2 \cos^2\left(\frac{\pi}{2} - \beta\right) \right]^{-1/2}$$

is for a spheroid, α_{abi}, α_{sci} are the coefficients of radiation absorption and scattering by the ith layer; S_s

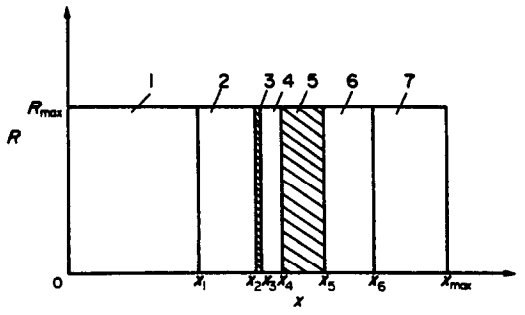

FIG. 1. The geometry of the model under consideration and the scheme of the eyeground layers: R, radial coordinate; x, coordinate along the axis of the cylindrical system of coordinates; 1, transport eye media; 2, neuroepithelium (retina); 3, pigment epithelium; 4, capillary layer of vascular membrane; 5, pigmented layer of vascular membrane; 6, vascular membrane; 7, sclera.

the area of particle cross-section, r_a, r_b the spheroid semiaxes, K_{ab}, K_{sc} the factors for efficiencies of radiation absorption and scattering by a particle, β the angle between the major axis of the spheroid and the x-axis. It should be noted that radiation in the PE heterogeneous layer should propagate based on the optics of scattering media [14]. It is shown in the latter work that the indicatrix of radiation scattering by particles with $r_0 \gtrsim 1/3\lambda$ is highly extended forward towards the incident radiation and has a sharp maximum at a zero scattering angle. In this case, in thin layers of about 100 μm the attenuation of radiation of the visible and near infrared ranges occurs exponentially only at the expense of radiation absorption [14] and it is possible to set $\alpha_{sc} \approx 0$ in equation (1).

While absorbing the energy of radiation, MPGs get heated and give up heat to the surrounding medium by heat conduction. The characteristic time of heat transfer for a granule with the radius $r_0 = 0.5$ μm (for spheroid the minor semiaxis should be taken) is evaluated by the equation

$$t_1 \sim \frac{r_0^2}{4\chi} \sim 4 \times 10^{-7}\,\text{s} \tag{2}$$

where χ is the thermal diffusivity of the medium [5]. The characteristic time of heat removal beyond PE of thickness $x_3 - x_2 = 5$ μm is

$$t_2 \sim \frac{(x_3 - x_2)^2}{4\chi} \sim 4 \times 10^{-5}\,\text{s}. \tag{3}$$

Here, two characteristic cases of the interaction of radiation with a granule can be distinguished: (1) when the characteristic time of heat exchange between a granule and the medium t_1, equation (2) is much smaller than the time of radiation pulse action $t_1 \ll t_p$ and (2) when $t_1 \gtrsim t_p$. Let the pulses in cases 1 and 2 be called long and short, respectively.

Consider the case $t_1 \ll t_p$. As shown in ref. [15], in this case the thermal balance equation of a single particle which absorbs the energy of radiation and emits it into the surrounding medium by means of non-linear heat conduction, in the approximation of a uniform temperature over the particle volume, has the form

$$V_0 \rho_0 C_0 \frac{\partial T_0}{\partial t} = K_{ab} I S_s - j_h S_0. \tag{4}$$

The thermal conductivity coefficient of the medium surrounding the particle is specified in the form

$$\kappa_i = \kappa_{i\infty} \left(\frac{T}{T_\infty}\right)^a \tag{5}$$

where $\kappa_{i\infty} = \kappa_i(T = T_\infty)$, $a = \text{const}$. Since the characteristic time needed to establish the temperature field around the particle t_1 is short relative to the duration of heating t_p, the heat exchange between the particle and the medium is considered in the quasi-stationary approximation [15]. The quasi-stationary heat transfer of a spherical particle with relation (5) taken into account was investigated in ref. [15] where for the temperature distributions around the particle $T(r)$ and j_h the following expressions were obtained, for example, at $a \neq -1$:

$$T(r) = T_m \left[1 + \frac{r_0}{r}\left\{\left(\frac{T_0}{T_m}\right)^{a+1} - 1\right\}\right]^{1/(a+1)} \tag{6}$$

$$j_h = -\kappa \left.\frac{dT}{dr}\right|_{r=r_0} = \frac{\kappa_{i\infty} T_m^{a+1}}{(a+1) T_\infty^a r_0}\left\{\left(\frac{T_0}{T_m}\right)^{a+1} - 1\right\}. \tag{7}$$

The quasi-stationary heat transfer of a spheroidal particle with relation (5) taken into account was investigated in ref. [16] where in the one-dimensional approximation with respect to ξ, $T = T(\xi)$ (ξ is the spheroidal coordinate) [17], the solution was obtained for the case under consideration, i.e. $a \neq -1$

$$T = T_m \left[1 + \frac{\ln \tanh \xi/2}{\ln \tanh \xi_0/2}\left\{\left(\frac{T_0}{T_m}\right)^{a+1} - 1\right\}\right]^{1/(a+1)} \tag{8}$$

$$j_h = -\frac{\kappa_{i\infty} T_m^{a+1} \arcsin(1/\cosh \xi_0)\{(T_0/T_m)^{a+1} - 1\}}{(a+1) c_s T_\infty^a \ln \tanh(\xi_0/2) \sinh \xi_0} \tag{9}$$

where $c_{sc} = \sqrt{(r_b^2 - r_a^2)}$, $r_b > r_a$, $\xi = \xi_0$ is the spheroidal surface. The two-dimensional non-stationary heat conduction equation for the entire volume of the laminated medium with the energy dissipation taken into account has the form

$$\rho_i C_i \frac{\partial T_m}{\partial t} = \frac{1}{R}\frac{\partial}{\partial R}\left(R \kappa_i(T_m) \frac{\partial T_m}{\partial R}\right) + \frac{\partial}{\partial x}\left(\kappa_i(T_m) \frac{\partial T_m}{\partial x}\right) + Q_i. \tag{10}$$

The distribution of radiation intensity across the section of the beam was assumed to be Gaussian. The radius R_{max} and the length x_{max} of the computational volume are selected in such a way as to preserve the initial conditions on its surface unperturbed within

the time interval considered. The heat source in expression (10) is prescribed in the form

$$i = 1,2,4,5, \quad Q_i = \alpha_{ab,i} I + \rho_i Q_d \frac{\partial f}{\partial t}$$

$$i = 3, \qquad Q_i = S_0 N_0 j_h + \rho_i Q_d \frac{\partial f}{\partial t} \qquad (11)$$

where Q_d is the specific heat of protein thermal denaturation (of about 25 J g^{-1} [18]), f the fraction of protein molecules which do not suffer thermal denaturation. The use of expression (11) means that the particles are assumed to be pointlike heat sources with identical temperature in a physically infinitesimal volume, with the volume occupied by the particles and heat aureolas around them (see equations (6), (9) and (7)) being much smaller than the volume of the surrounding medium. The initial and boundary conditions for equations (1) and (4)–(10) will be

$$I(x = 0, R) = I_0 \exp(-R^2/R_b^2), \quad 0 \leqslant t \leqslant t_p;$$
$$I = 0, \; t > t_p; \quad T_0(x, R, t = 0) = T_\infty;$$
$$T_m(x, R, t = 0) = T_\infty; \quad T_m(R = R_{max}) = T_\infty;$$
$$T_m(x = 0) = T_\infty; \quad T_m(x = x_{max}) = T_\infty;$$
$$\left.\frac{\partial T_m}{\partial R}\right|_{R=0} = 0. \qquad (12)$$

The system of equations (1) and (4)–(9) with initial and boundary conditions (12) allows the space–time temperature fields in biotissue to be calculated with the granular structure of the pigmented layer for $t_p \gg t_1$ taken into account.

Consider the case $t_p \lesssim t_1$ when the essential feature of particle heating by optical radiation is a non-stationary character of its heat exchange with the surrounding medium [15, 16]. Therefore, in this case the energy release and heat exchange between a granule and the surrounding medium is represented by the non-stationary heat-conduction equation, which for spherical particles has the form

$$C\rho \frac{\partial T}{\partial t} = \frac{1}{r^2}\frac{\partial}{\partial r}\left(\kappa r^2 \frac{\partial T}{\partial r}\right) + q \qquad (13)$$

and for spheroidal particles in the one-dimensional approximation with respect to ξ [16] has the form

$$c_*^2 \sinh\xi(\cosh^2\xi - \tfrac{1}{3})C\rho\frac{\partial T}{\partial t} = \frac{\partial}{\partial \xi}\left[\sinh\xi\kappa\frac{\partial T}{\partial \xi}\right]$$
$$+ c_*^2 \sinh\xi(\cosh^2\xi - \tfrac{1}{3})q. \qquad (14)$$

Here c, ρ and κ are the heat capacity, density and thermal conductivity of the particle substance for $r \leqslant r_0(\xi \leqslant \xi_0)$ and of the surrounding medium substance for $r > r_0(\xi > \xi_0)$, q the power density of the energy release by a particle at the expense of radiation energy absorption and energy losses for protein thermal denaturation

$$q = \frac{IK_{ab}S_*}{V_0} + \rho Q_d \frac{\partial f}{\partial t}, \quad r \leqslant r_0 \qquad (15)$$

beyond the particle

$$q = \rho Q_d \frac{\partial f}{\partial t}, \quad r > r_0.$$

The temperatures of the medium and particle coincide on their interfaces. The initial and boundary conditions for relations (13) have the form

$$T(r, T = 0) = T_\infty; \quad \left.\frac{\partial T}{\partial r}\right|_{r=0} = 0$$
$$\left.\frac{\partial T}{\partial r}\right|_{r=r_c} = 0 \quad \text{for } t \leqslant t_1,$$
$$T(r = r_c, t) = T_m \quad \text{for } t > t_1. \qquad (16)$$

Similarly for expression (14)

$$T(\xi, t = 0) = T_\infty; \quad \left.\frac{\partial T}{\partial \xi}\right|_{\xi=0} = 0$$
$$\left.\frac{\partial T}{\partial \xi}\right|_{\xi=\xi_c} = 0 \quad \text{for } t \leqslant t_1,$$
$$T(\xi = \xi_c, t) = T_m \quad \text{for } t > t_1. \qquad (17)$$

Here $r = r_c$ and $\xi = \xi_c$ are the boundaries of spherical and spheroidal cells into which the entire volume PE is divided. The cell centres are occupied by granules, whereas their remaining volume, determined as $1/N_0$, is filled with the surrounding medium. Saying that

$$t_p \lesssim t_1 \ll t_2 \qquad (18)$$

enables the entire process to be divided into several stages. When $t \lesssim t_1$, the granules are heated during the pulse, then they cool off and heat their surroundings. This process is described by equations (13)–(17), in the approximation of thermally insulated cells, and is terminated with temperature equilibration inside the PE cells at $t \sim t_1$. When $t > t_1$, the heat removal from PE into adjacent layers begins and this process is described in the system of equations (10)–(12). The resulting space–time temperature distributions were used to calculate the degree of thermochemical transformations (TCT), i.e. the fractions of molecules which suffer thermal denaturation, by the kinetic equation [1]

$$\frac{\partial f}{\partial t} = -\frac{k_B T}{h}\exp\left(-\frac{\Delta H - T\Delta S}{R_g T}\right) f \qquad (19)$$

under the initial condition

$$f(x, R, t = 0) = 1. \qquad (20)$$

Thermal denaturation is the heating-induced breakdown of the structure of a protein macromolecule leading to the loss by protein of natural functional properties [18]. The solution of the system of equations (1)–(20) was made numerically [19, 20].

3. THERMAL PROCESSES DURING THE INTERACTION OF LONG OPTICAL RADIATION PULSES WITH THE EYEGROUND TISSUES

Consider thermal processes occurring during the interaction between long radiation pulses with $\lambda = 0.514$ μm and the eyeground biotissues when $t_1 \ll t_p$ (see equation (2)) [21, 22]. In this case thermal and thermochemical processes in the eyeground tissue are described by the system of equations (1), (4)–(11) and (19) with the initial and boundary conditions (12) and (20). Use was made of the following values of parameters: the radius of a spherical pigmented granule $r_0 = 1$ μm, $N_0 = 3.58 \times 10^{16}$ m^{-3}, $K_{ab} = 1.34$, $a = 0.66$ [23], $T_\infty = 310$ K, ΔH, ΔS are taken from ref. [8].

The incident radiation energy is absorbed selectively by pigmented granules in PE, with the absorption by the surrounding medium being much weaker. Therefore, during the irradiation the temperature of the granules exceeds that of the surrounding medium. The characteristic time of heat transfer for the granules with radius $r_0 \sim 1$ μm can be evaluated by the formula $t_1 \sim r_0^2/4\chi \sim 1.4 \times 10^{-6}$ s (see equation (2)). Consequently, when $t_p \gg t_1$, the radiation pulse interacts with the heterogeneous medium under the conditions of a developed heat exchange between the heated particles and the surrounding medium and general temperature increase.

The processes in heterogeneous laminated media were calculated for the threshold energy density $E_{0t} = 1.8 \times 10^3$ J m^{-2}, $t_p = 10^{-4}$ s, $R_b = 140$ μm taken from the experimental study in ref. [24]. Figure 2(a) shows the behaviour of the temperature of the granules and medium at several points in space. Immediately after the beginning of the irradiation the heating of the granules and their heat exchange with the surrounding medium start. The excess heating of the granules with respect to the medium reaches a maximum of about 8–10 K and depends on the local value of the intensity, size and optical characteristics of the particles, etc. At $x = x_2$ the particles get heated more rapidly than in the case of $x > x_2$, when the particles are acted upon by weaker radiation attenuated by the medium. However, during the formation of a characteristic temperature profile (see Fig. 3) resulting from the simultaneous heating by radiation and cooling by heat conduction the temperature maxima of the granules and medium move towards the interior of the PE layer. After the radiation is turned off, the granules give up energy to the medium for about 5×10^{-6} s and their temperature T_0 becomes equal to T_m. The time of thermal relaxation of the granules of about 5×10^{-6} s agrees with the given evaluation of the characteristic heat transfer time t_1.

Figure 2(b) presents the distributions of T_0, T_m, f, $z_1 = I(x, R)/I_0$ along R in the planes $x = x_2$, $x_2 + 2$ μm for several time instants. In the case under consideration the characteristic radius of the beam R_b exceeds by an appreciable factor the thickness of the

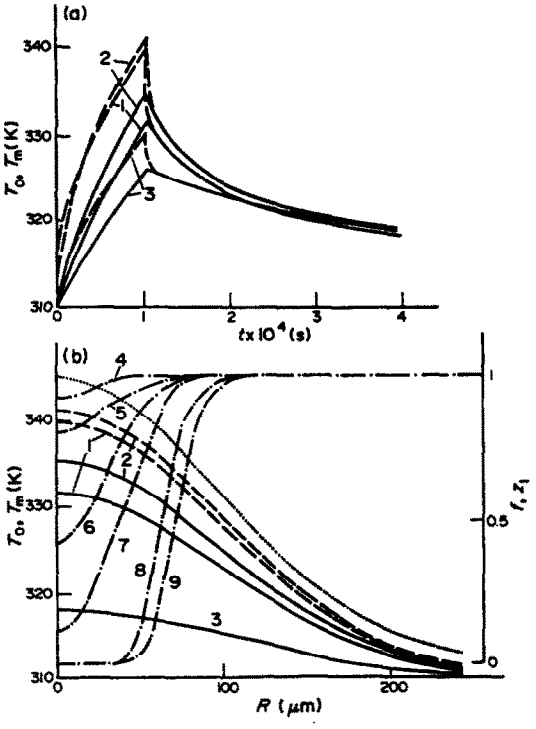

FIG. 2. Dependence of the medium T_m (——) and granule T_0 (– – –) temperatures at the points $R = 0$, $x = x_2(1), x_2 + 2$ μm (2), x_3 (3) on t (a) and on the degree of thermochemical transformations f (– · – · –) along R for the medium directly at the granule surface (8, 9) and at a distance from granules (4–7) for $t = 10^{-4}$ (1, 2, 4, 6, 8, 9), 6×10^{-4} s (3, 5, 7–9) and in the cross-sections $x = x_2$ (1, 3–5, 8), $x_2 + 2$ μm (2, 3, 6, 7, 9). The distribution of the normalized radiation intensity z_1 along R at $x = x_2$ for $0 \leqslant t \leqslant t_p$ (· · · · ·) (b).

absorbing layer $x_3 - x_2$. Therefore, a substantial heating of the regions adjacent to the layer $x_3 - x_2$ occurs along the longitudinal x-axis and, to a lesser degree, of the medium in the radial direction. With an increase of R (decrease of I) both the temperature of the granules and the medium and the difference between them decrease. The region with volume TCT expands appreciably in the radial direction when the pulse is terminated during the cooling of the heated region. The rate of thermochemical reactions, equation (19), depends strongly on temperature and is of threshold character. The heating (or temperature decrease) below 330–340 K at the given ΔH and ΔS leads to the absence (or abrupt retardation) of reactions for the above-indicated time intervals. A considerable difference between the temperatures of the granules and of the medium during the pulse can bring about the difference in the rates of reactions directly at the surface of the granules with the temperature T_0 and in the medium with the temperature T_m. This can result in the regime of selective interaction, when thermodynamical reactions proceed inside and in the immediate vicinity of the surface of the heated granules and when they are absent in the remaining volume of the medium [25, 26], i.e. the TCT microregions are located inside and around the granules. In the present

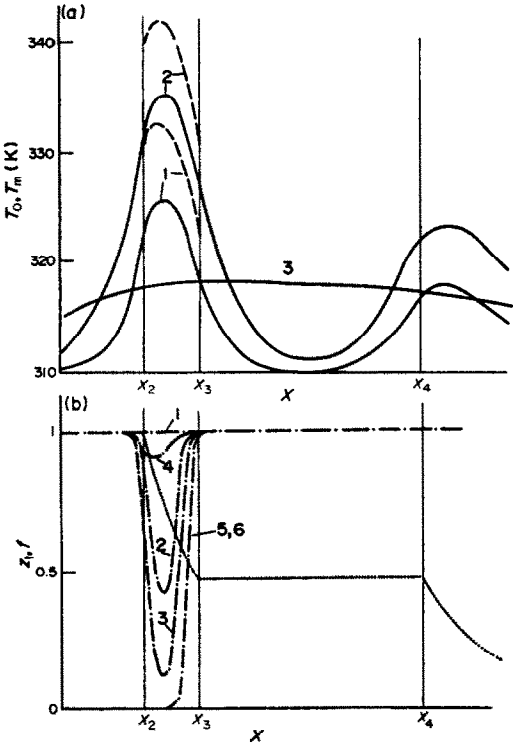

FIG. 3. The distributions of T_0 (– – –) and T_m (——) along x at $R = 0$ for $t = 0.5 \times 10^{-4}$ (1), 1×10^{-4} (2), 6×10^{-4} s (3) (a) and the distributions of f (– · – · –) for the medium at the granule surface (4–6) and at a distance from it (1–3) for $t = 0.5 \times 10^{-4}$ (1, 4), 1×10^{-4} (2, 5), 6×10^{-4} s (3, 6). The distribution of z_1 along x at $R = 0$ for $0 \leqslant t \leqslant t_p$ (· · · · ·) (b).

case when irradiation occurs with the threshold energy [24], along with the TCT macroregion of characteristic sizes of about 30–50 μm, a vast region with selective interaction is observed. In Fig. 2(b) the boundary of the region is marked, in which TCT proceeds directly at the surface of the granules. In the space between the boundaries of the regions with volume and surface TCTs the microregions broaden until they completely join on the TCT macroregion boundary. It should be noted that under the action of the pulses of length $t_p = 10^{-5}$–10^{-3} s and below-threshold energy density $E_0 = (0.5-0.8)E_{0t}$ selective interaction with granules is realized which causes TCT of the proteins inside the granules and in the direct vicinity of their surfaces without forming a continuous macroregion of transformations.

In Figs. 3(a) and (b) the distributions of T_0 within the PE layer, $x_3 - x_2$ and also T_m, f and z_1 along x at $R = 0$ are plotted for several instants of time. During the action of a pulse the energy of irradiation is absorbed by the layers $x_3 - x_2$, $x_5 - x_4$ and it is actually not absorbed in the layers $x_2 - x_1$, $x_4 - x_3$, $x_6 - x_5$. This leads to an appreciable heating of the particles and medium in the layer $x_3 - x_2$ and to a weaker (due to radiation attenuation) heating of the layer $x_5 - x_4$. As a result, in the course of the two-dimensional unsteady heat exchange between the heated layers and the surrounding medium, a characteristic temperature distribution is formed being subsequently cooled after termination of the radiation pulse. In the layer $x_3 - x_2$ the region of continuous TCTs is established and also a broader region of transformations proceeding directly at the surface of the granules. The maximum excess heating of the medium at the point $x_2 + 2$ μm, $R = 0$, calculated for the experiments of ref. [24] at $R_b = 140$ μm is, on average, equal to 25–30 K and almost does not depend on t_p in the time interval 10^{-3}–10^{-4} s.

Figure 4(a) shows the heating isotherms for the medium $\Delta T_m = T_m - T_\infty = 20$ K and granules $\Delta T_0 = T_0 - T_\infty = 20$ K and also the lines of TCT constant degree for the molecules of the medium $f = 0.5$ for several time instants. During heat transfer and cooling when $t > t_p$ the macroregion of TCTs with $f < 0.5$ broadens considerably. At the same time, the region of transformations in the immediate vicinity of the surface of the granules conserves a constant form when $t > t_p$, because no noticeable TCTs take place for the characteristic time of the thermal relaxation of granules $t_1 \sim 10^{-6}$–10^{-5} s.

Figure 4(b) presents the excess heating of particles ΔT_0 with respect to the medium at the point $x = x_2$,

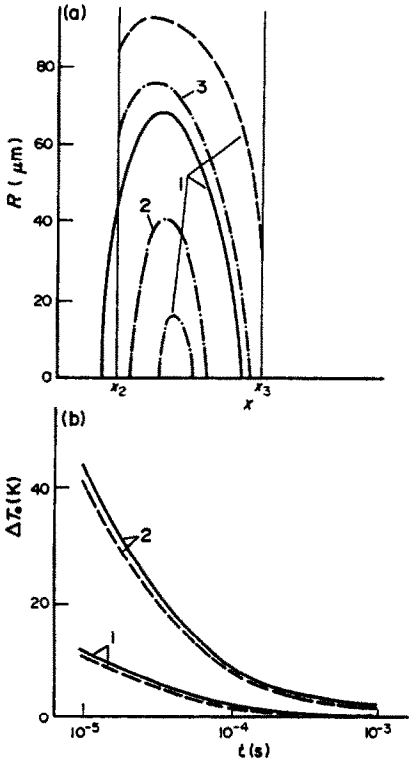

FIG. 4. The heating isotherms of the medium $\Delta T_m = 20$ K (——), granules $\Delta T_0 = 20$ K (– – –) and equal TCT level $f = 0.5$ (– · – · –) on particles (3) and in the medium (1, 2) for $t = 1 \times 10^{-4}$ (1, 3), 6×10^{-4} s (2, 3) and the dependence of $\Delta T_0 = T - T_m$ on t_p for spherical particles (——) with $r_0 = 0.5$ (1), 1 μm (2) and spheroids of the same volume (– – –) (1, 2), respectively (b).

$R = 0$ calculated for $R_b = 140$ μm at $t_p = 10^{-3}$, 5×10^{-4}, 1×10^{-4} s for the conditions of ref. [24]; when $t_p = 10^{-5}$ s the value $E_0 = 1 \times 10^3$ J m^{-2} is taken. Under the threshold conditions the excess heating of granules ΔT_0 increases sharply with decrease of t_p and amounts to about 45 K at $t_p = 10^{-5}$ s. In this case for $t_p = 10^{-3}$ s the excess heating ΔT_0 is equal to about 1–3 K. Consequently, for the radiation pulses of length $t_p > 10^{-3}$ s and threshold and below-threshold intensity the excess heating of the granules ΔT_0 will not exceed 1–2 K and thermal processes can be described in the quasi-homogeneous approximation without taking into account the granules. However, under the conditions of threshold and below-threshold irradiation with $t_p < 10^{-3}$ s and over-threshold irradiation with $t_p \geq 10^{-3}$ s the heterogeneous structure of the absorbing layers should be taken into account. It should be noted that the possibility of predicting thermal processes in heterogeneous layers in the quasi-homogeneous approximation should be analysed on a case-by-case basis.

To clarify the effects of the sizes of granules on their excess heating with respect to the medium, consider the values of ΔT_0 at the point $x = x_2$, $R = 0$ calculated for the parameters E_0, t_p [24] but at $r_0 = 0.5$ μm, $N_0 = 2.86 \times 10^{17}$ m^{-3}, $K_{ab} = 0.67$ and the same optical parameters of the PE layer and volume filling of the layer by granules. The qualitative behaviour of ΔT_0, T_0, T_m (see Fig. 4(b)) remains unchanged but the excess heating ΔT_0 of the granules at $r_0 = 0.5$ μm is smaller than at $r_0 = 1$ μm since the energy absorbed by the granules decreases with a decreasing radius. In this case the heating of the medium does not actually change and, correspondingly, the properties and final dimensions of the TCT macroregion remain the same. At the same time the decrease in the excess heating of the granules substantially reduces the size of the region in which the TCT microregions appear inside and around the granules, and can cause its total disappearance. Thus, the size of granules can essentially affect the excess heating with respect to the medium. As r_0 grows, ΔT_0 increases, whereas with a decrease of r_0 the value of ΔT_0 also decreases and the properties of the heterogeneous medium approach the properties of the homogeneous media.

To investigate the effect of the shape of particles on thermal processes, the interaction of radiation pulses with laminated media was calculated numerically when the layer $x_3 - x_2$ contained a collection of identical spheroids with $r_a = 0.415$ μm, $r_b = 0.725$ μm and $r_a = 0.830$ μm, $r_b = 1.45$ μm provided the optical parameters of the heterogeneous layer and the volume filled with granules remained unchanged and the volumes of the spheroids and spherical granules with $r_0 = 0.5$ μm, respectively, were equal. In Fig. 4(b) the excess heating of spheroidal particles ΔT_0 is plotted vs t_p, calculated for the conditions of the experiments of ref. [24]. For spheroidal particles, the excess heating is lower by 1–3 K than for spherical particles of the same volume. This is due to an increase of the heat flux away from the spheroid. Otherwise, the qualitative and quantitative pictures of the interaction process remain practically unchanged.

It is known that in a medium which suffers TCT changes its optical properties, in particular, its reflection coefficient for the radiation increase [27]. The time interval after the termination of which the optical properties change was determined experimentally in ref. [27] and was found to be equal to 5–500 ms, on average to about 50 ms. In the present case the duration of pulses $t_p = 10^{-5}$–10^{-3} s is much smaller than 50 ms and variation of the medium optical properties during the pulse of radiation can be neglected.

4. THERMAL PROCESSES DURING THE INTERACTION OF SHORT OPTICAL RADIATION PULSES WITH THE EYEGROUND TISSUES

Consider thermal processes occurring during the exposure of the eyeground tissue to short optical radiation pulses when $t_p \lesssim t_1$ (see equation (2)) [21, 26, 28]. In this case thermal and thermochemical processes in the eyeground tissues are represented by the system of equations (1), (10), (13), (14) and (19) with boundary conditions (12), (16), (17) and (20). The approximate numerical methods applied make it possible to calculate the interaction of laser radiation pulses of length $t_p \lesssim 10^{-6}$ s and to obtain the pattern of thermochemical transformations inside and around separate granules, and also throughout the entire volume of biotissue under consideration.

The interaction between the radiation pulse of length $t_p = 1 \times 10^{-8}$ s with the energy density on the beam axis $E_0 = 0.26$ J cm^{-2} and $\lambda = 0.694$ μm, and the eyeground biotissues, when the diameter of the image on the retina $D_b = 2R_b = 30$ μm, was calculated numerically by the radiation intensity level $I_0 \times \exp(-1)$. Considered for $N_0 = 2.87 \times 10^{17}$ m^{-3} were: the case of spherical granules with radius $r_0 = 0.5$ μm, with the radius of the spherical cell which contains the granule being $r_c = 0.94$ μm, and the case of spheroidal granules the volume of which is equivalent to that of spherical granules with the semi-axes of the ellipsoid $r_b = 0.676$ μm, $r_a = 0.430$ μm. Spheroidal coordinates [17] corresponding to the boundary of the granule and to that of the spheroidal cell are equal to $\xi_0 = 0.75$ and 1.31, respectively.

Figure 5(a) gives the distributions of the temperature T and of the fraction f of protein molecules, which did not suffer thermochemical transformations (thermal denaturation), within the cell on the beam axis at the point $x = x_2 + 2$ μm for a spherical granule and radiation pulse length $t_p = 10^{-8}$ s. The radiation pulse causes an intensive heating of the granule, with the temperature inside it being virtually independent of the coordinate and the temperature drop being observed only in the surface layer of the granule and in the adjacent layer of the surrounding medium. The cooling of the granule is accompanied by the heat

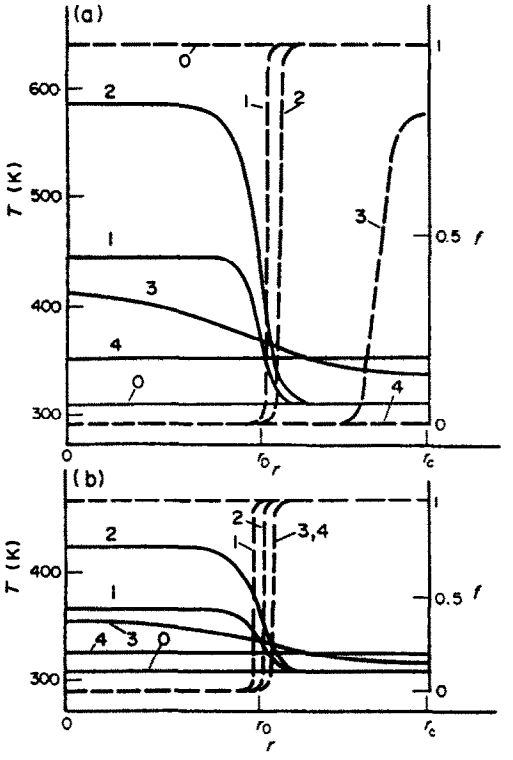

FIG. 5. The distribution of the temperature T (——) and of the fraction f of protein molecules, which did not suffer thermochemical transformations (– – –), along the radius r within the cell for the time instants $t = 0$ (0), 5×10^{-9} (1), 1×10^{-8} (2), 5×10^{-7} (3), 1.76×10^{-6} s (4) at the pulse length $t_p = 1 \times 10^{-8}$ s, energy $E_0 = 0.26$ J cm^{-2} (a) and $E_0 = 0.11$ J cm^{-2} (b). A spherical granule with $r_0 = 0.5$ μm and $r_c = 0.94$ μm.

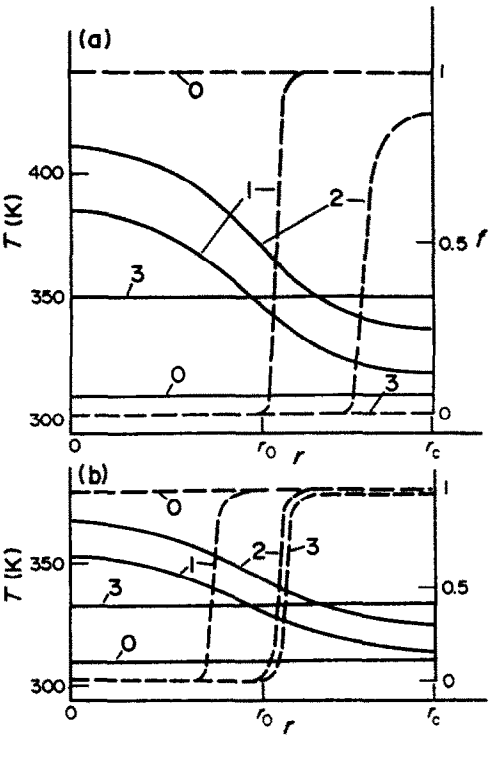

FIG. 6. The distribution of the temperature T (——) and of the fraction f of protein molecules, which did not suffer TCT (– – –), along the radius r within the cell for the time instants $t = 0$ (0), 5×10^{-7} (1), 1×10^{-6} (2), 1.7×10^{-6} s (3) at $t_p = 1 \times 10^{-6}$ s, $E_0 = 0.26$ J cm^{-2} (a) and $E_0 = 0.15$ J cm^{-2} (b). A spherical granule with $r_0 = 0.5$ μm and $r_c = 0.94$ μm.

wave and the wave of thermochemical transformations propagating from it in the surrounding tissues. As compared with the spheroidal granule there is only a more rapid equilibration of temperature within the limits of the latter attributable to its more intense heat exchange with the surrounding medium due to a larger surface area at the same volumes. Figure 6(a) presents the distributions of T and f within the cell on the beam axis at the point $x = x_2 + 2$ μm for $t_p = 10^{-6}$ s. Here, the specific feature of radiation interaction with a granule is the presence of its developed heat transfer with the surroundings already during the pulse action. It can be noted that the temperature profile, which takes a certain form after the lapse of some time from the start of irradiation, rises uniformly with time without changing it, up to termination of the radiation pulse. The time for temperature equilibration within the cell appears to be practically the same as that for the pulse $t_p = 10^{-8}$ s. Thus, the laser radiation energy is absorbed selectively by pigment particles (MPGs) leading to their heating considerably in excess of the surrounding medium and to the propagation of the wave of thermochemical transformations from their surface into the surrounding tissues in the process of heat exchange. In Figs. 5(a), 6(a) and 7 the results of the variants are given calculated from the experimental data of ref. [29]. In this case a complete denaturation of protein molecules occurring throughout the entire volume of the cells, turned out to be near the beam axis resulting in the formation of a continuous macroregion with a diameter of about 24–25 μm (see Fig. 7). This kind of denaturation focus can be interpreted as that visualized ophthalmoscopically [4, 29]. It should be noted, however, that the denaturation reaction rate depends strongly on temperature (see equation (19)) and the cooling of biotissue below 330–340 K causes an abrupt retardation of the reaction and, further, the ceasing of the denaturation region expansion during the above-indicated intervals of time. Therefore, such irradiation regimes can be obviously realized with a decreasing radiation pulse energy (intensity) under which denaturation microregions inside and around pigment granules can be formed which would not overlap one another due to a strong temperature dependence of the protein denaturation rate, equation (19). In Figs. 5(b) and 6(b) the distributions of T and f within the previously considered cells are given at the energy densities $E_0 = 0.11$ J cm^{-2} for $t_p = 10^{-8}$ s and $E_0 = 0.15$ J cm^{-2} for $t_p = 10^{-6}$ s. In this case complete denaturation is suffered by the proteins in the granule itself and in the 0.5 μm thick spherical layer directly

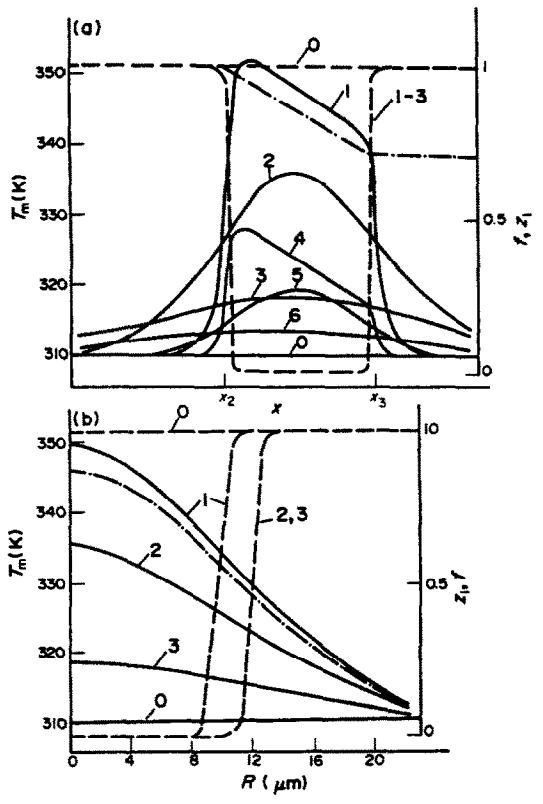

FIG. 7. The distributions of T_m (——) and f (– – –) at $R = 0$ (1–3) and $R = R_b = 0.15$ μm (4–6) for the time instants $t = 0$ (0), 1.76×10^{-6} (1,4), 5×10^{-5} (2,5), 2×10^{-4} s (3,6) and z_1 ($R = 0$) (– · – · –) during the pulse action along the coordinate x (a) and the coordinate R for $x = x_2 + 2$ μm (b), $\lambda = 0.694$ μm.

adjacent to the granule. In the remaining volume of the cell the protein denaturation is virtually not observed. Consequently, denaturation (coagulation) microregions can originate in the eyeground tissues under radiation intensities less than about 2–3 times the threshold ones determined ophthalmoscopically. It should be noted that as the pulse duration increases, the difference between the energies necessary to obtain the impairment visualized ophthalmoscopically and microdamages on the granules decreases. The fact that microdamages can appear without being detected by the standard ophthalmoscopical methods is confirmed by the experimental data of ref. [30], in which the special procedure allowed the changes in the eyeground to be detected at the energies half as large as the threshold ones. At the same time, calculations by the method of refs. [5–9] carried out without taking into account the PE granular structure did not give denaturation regions at $E_0 = 0.15$ J cm^{-2}.

Thus, taking into account the granular structure of pigmented biotissues (for example, of the eyeground, skin and other biotissues) opens the possibility for the selective interaction of radiation with biotissues and for the formation of protein denaturation microregions inside and around the pigmented granule at radiation intensities 2–3 times less than experimental threshold intensities. This fact should be taken into account when setting up safety norms for short radiation pulses. On the other hand, the formation of denaturation (coagulation) microregions around pigment particles allows selective irradiation of cells and separate parts of biotissue cells. The thickness of the denaturation region around the pigment granule can be varied by corresponding selection of radiation intensity. The method of selective irradiation of pigmented biotissues can be used for coagulating pigmented tumors, in microsurgery of the eyeground tissues, neurosurgery, etc. The selective irradiation effect can be enhanced substantially by staining the biotissues to be coagulated by the laser radiation pulse.

5. EFFECT OF DIFFRACTION ON THE OPTICAL RADIATION BEAM INTENSITY DISTRIBUTION AND ON THE DEGREE OF THERMOCHEMICAL TRANSFORMATIONS

In theoretical and experimental studies on the interaction of optical radiation beams with the eyeground tissues (the retina) [6–12] the Gaussian intensity distribution on the retina is usually assumed $I = I_0 \times \exp(-R^2/R_b^2)$. However, no account is being taken of the possibility of radiation beam diffraction on the circular aperture (pupil or the exit of the radiator). Taking into account the radiation beam diffraction aperture can appreciably change the radiation intensity distribution on the retina. The distribution of the optical radiation beam intensity on the retina with regard for diffraction and the effect of this factor on the distribution of degrees of thermochemical transformations in the retina proteins are of considerable interest and will be considered in the present section.

Examine the formation of radiation intensity distribution on the retina when the cornea is hit by a collimated radiation beam with a certain intensity distribution I over the cross-section. Let the beam diffraction proceed on the circular aperture (the exit pupil of a radiator adjacent directly to the cornea) with the diameter D_0 equal to about 5 mm, because the typical eye pupil diameter does not exceed 5 mm and, moreover, because in ophthalmology the radiation beams with the diameter $D_0 < 5$ mm are employed to avert the iris damage. In this case, when $D_0 < 5$ mm, spherical and chromatic aberrations of the eye can be neglected [31]. This approximation is widely applied when studying diffraction problems [33]. A simplified optical eye [31, 32] consists of a positive lens followed by a vitreous body with the refraction index $n = 1.336$. It is assumed that the front and rear main planes of the eye are mated with the plane of the pupil (aperture). For the spot size $\leqslant 0.1$ μm, the retina surface within the spot can be considered flat with good accuracy. Numerical values of the parameters for a schematic normal eye are taken from ref. [32].

The propagation of a limited radiation beam in the eye media will be described by the parabolic equation of quasioptics [33]

$$2ik\frac{\partial A}{\partial x} = \Delta_\perp A - ik\alpha A \tag{21}$$

where $k = 2\pi/\lambda$, λ is the wavelength of monochromatic radiation propagating along the x-axis, A the complex amplitude of the electromagnetic field electric vector $I = A \cdot A^*$, $\Delta_\perp = \partial^2/\partial y^2 + \partial^2/\partial z^2$; x, y, z are the axes of the Cartesian coordinate system, α the coefficient of radiation attenuation by eye media for $x < x_1$. The possibility for the use of parabolic equation (21) is provided by the narrow angular spectrum of the beam which propagates mainly within the cone, the angle at the apex of which does not exceed 13°. The boundary condition at $x = 0$ is prescribed in the form of the Gaussian and uniform distributions for the amplitude A within the aperture of radius $R_0 = D_0/2$:

for $R = \sqrt{(y^2+z^2)} \leqslant R_0$

$$A(x=0,y,z) = A_0 \exp\left(-\frac{R^2}{2R_0^2} - ik\frac{R^2}{2F}\right) \tag{22}$$

or

$$A(x=0,y,z) = A_0 \exp\left(-ik\frac{R^2}{2F}\right) \tag{23}$$

for $R > R_0$

$$A(x=0,y,z) = 0$$

where A_0 is the amplitude of the electric vector of the wave at $x = y = z = 0$, F the radius of the wave front curvature, i.e. the focal length of the optical system. The system of equations (21)–(23) was solved numerically by the Fourier fast transformation technique [34]. Equation (21) does not involve the self-induced thermal blooming of the beam, because for visible and near infrared radiation ranges the coefficient of radiation attenuation by transparent eye media does not exceed 0.1–0.3 cm^{-1} and, for the most part, is due to scattering [36]. At the same time, it seems that in the case of infrared radiation propagation with high absorption coefficient and sharp beam focusing, the self-induced thermal blooming of the beam should be taken into account.

The diffraction of the radiation beam on an aperture is the classical field of optics [31, 32] which recently has been in rapid development in connection with the investigations into the diffraction of laser beams [33–35]. The radiation beam diffraction in the eye media has, however, a number of spherical features, namely the focusing of a limited beam with some intensity distribution over the cross-section and the study of the image near the focal plane. That equation (1) for the region near the focal plane could be solved numerically, with the necessary accuracy and space resolution, use was made of the adapting system of coordinates based on Talanov's transformation [34]. The reduction of the computational grid along the coordinates y, z is determined by the geometric convergence of the beam. For checking the accuracy of the computational procedure, the diffraction on a circular aperture was calculated and the results obtained were compared with experiments [31, 35]. A very good coincidence was achieved on the grids with 256×256 points along the coordinates y, z.

To consider the radiation intensity distribution in the plane $x = \text{const.}$, it is convenient to employ the normalized intensity I_n/I_{max} and radius $R_n = R/R_b(x)$, where $I_{max} = e^{-\alpha x} I_0 (R_0/R_b)^2$, $R_b(x)$ is the characteristic radius determined by the geometric convergence of the beam

$$R_b(x) = R_0\left(1 - \frac{x}{F}\right) \quad \text{for } x < F$$

$$R_b(x) = R_0\left(\frac{x}{F} - 1\right) \quad \text{for } x > F. \tag{24}$$

Parabolic equation (1) is valid for $R(x) \gg \lambda$, therefore the interval $F - x_F < x < F + x_F$, where x_F is determined from the condition $R_b(F - x_F)$, $R_b(F + x_F) \gg \lambda$, does not fall into the region under consideration. The distribution of I_n along R_n within this interval range, i.e. when $x \sim F$, can be found from the solutions obtained in refs. [31, 32]. Beyond the interval indicated, the solution is determined completely by the number of Fresnel zones Φ fitted into the entry aperture and is found numerically. Φ is obtained from the relations

$$\Phi = \frac{R_0^2 n}{\lambda}\left(\frac{1}{x} - \frac{1}{F}\right) \quad \text{for } x < F$$

$$\Phi = \frac{R_0^2 n}{\lambda}\left(\frac{1}{F} - \frac{1}{x}\right) \quad \text{for } x > F. \tag{25}$$

Figure 8 gives the distributions of I_n along the radius R_n calculated at the Fresnel number $\Phi = 5$ for uniform and Gaussian radiation intensity distributions with respect to the radius of the entry aperture. When the Fresnel numbers are low, considerable drops between the maxima and minima of the intensity are observed. As the Fresnel number increases, the number of diffraction maxima grows, whereas the relative drops between the maxima and minima diminish. The uniform intensity distribution leads to more appreciable drops. These features of intensity distribution over the retina are confirmed experimentally [37]. Moreover, Fig. 8 presents for comparison the initial uniform and Gaussian intensity distribution over the aperture. It is seen, that it is possible to describe the intensity distribution over the spot on the retina by the distribution similar to the initial distribution over the cornea. When $\Phi \gtrsim 10$, the mean error can amount to about 30% for the initial Gaussian distribution and about 50% for a uniform initial distribution, the mean error decreasing with an increase in Φ.

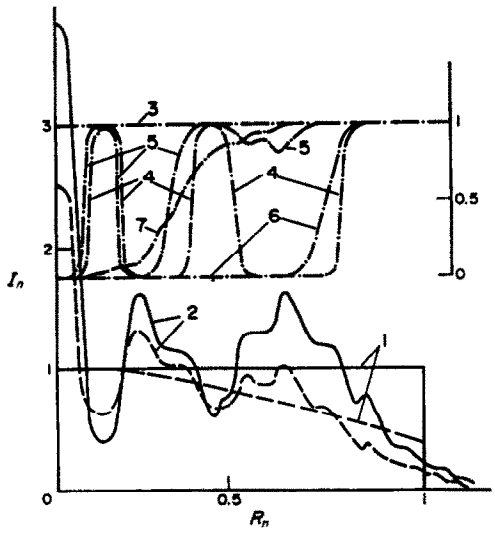

FIG. 8. The distributions of $I_n(R_n)$ over the cornea (1) and retina (2) for the uniform (——) and Gaussian (– – –) initial intensity distributions over the cornea and f (– · – · –) along R_n at $t = 0$ (3) and after the pulse action with $t_p = 10^{-4}$ (4, 5), 10^{-2} s (6, 7) for the uniform (4, 6) and Gaussian (5, 7) initial intensity distributions over the cornea at $\Phi = 5$.

In order to clarify the effect of the inhomogeneities in the distribution of $I_n(R_n)$ on the processes of radiation interaction with the eyeground tissues when diffraction effects are taken into account, the calculations of thermochemical denaturation of the retina proteins were carried out using the $I_n(R_n)$ distributions obtained. The calculations were conducted by the available techniques for $\lambda = 1.06$ μm and $\Phi = 5$ and for the constant characteristic radiation beam radius on the retina $R_b = 150$ μm. The radiation pulse energies were selected such as to obtain threshold focuses, i.e. such spatial regions in which the fraction f of molecules having not suffered thermochemical transformations (denaturation) decreased from the initial value $f(x, y, z, t = 0) = 1$ to $f \leqslant 0.1$. The intensities I_0 for the uniform and Gaussian distributions were taken to be identical at the fixed pulse length t_p. Figure 8 presents the distributions of f along R_n at $x = x_2 + 2$ μm after the termination of thermochemical transformations for the variants with $t_p = 10^{-4}$ and 10^{-2} s. When $t_p \leqslant 10^{-4}$ s, the distributions of the fraction of molecules f and of the temperature of biotissues at the instant of pulse termination T qualitatively repeat the distribution of $I_n(R_n)$, with the maximum of T and minimum of f values corresponding to the maximum value of I_n. In the case of short pulses with threshold energies, heat conduction almost does not affect the distribution of f. However, when the pulses are long or the radiation energy exceeds the threshold of heat exchange between the heated regions and the surrounding biotissues, the heat conduction leads to the thermochemical denaturation over the entire volume of the tissue and to the formation of a continuous denaturation focus with a certain distribution of f along the radius. Figure 8 presents the distributions of f at $t_p = 10^{-2}$ s which illustrate the aforegoing. The formation of a similar continuous denaturation focus at $t_p = 10^{-2}$ s was also observed at $\Phi = 10$ and above, but this is not shown in Fig. 8.

Thus, taking into account the diffraction effects when investigating the denaturation of the retina proteins enables the thermodenaturation regions separated by a non-damaged or partially damaged tissue, with the regions of maximum thermochemical transformations being localized in accordance with those of the radiation intensity maxima to be obtained.

It should be noted that the restriction of a radiation beam by a rigid aperture can cause, even at relatively low radiation intensities, considerable intensity oscillations in the image field. The diffractional maxima of the intensity can induce local excess heating of biotissue with subsequent ruptures, haemorrhages, formation of blisters, etc. which should be taken into account in ophthalmologic practice. The energy redistribution over the beam cross-section due to diffraction should also be taken into account when setting up safety norms for handling intensive light sources. To eliminate or diminish the diffraction effect, it is necessary to restrict the beam at the minimal intensity level possible, and also to use soft aperture, beam apodization and so on. The computational results show that the application of the above methods provides an appreciable attenuation of diffraction effects.

6. CONCLUSION

Thus, the paper was concerned with theoretical investigation of energy absorption, heat exchange and thermochemical processes during the interaction of optical radiation pulses with pigmented spherical and spheroidal granules in heterogeneous laminated biotissues. Numerical solution of the system of equations set gave the space–time temperature distributions, degree of thermochemical transformations of biotissue molecules inside and around the pigmented granules and in the volumes of laminated biotissues. The possibility for selective interaction of short radiation pulses with pigmented biotissues is shown which consists in the formation of thermodenaturation microregions inside and around the pigmented granules. The effect of diffraction on the distribution of optical radiation beam intensity is studied and the possibility for the formation of thermodenaturation regions separated by a non-damaged biotissue is shown. The results obtained are of interest for studies of thermal interaction of optical radiation with heterogeneous biotissues in photobiology and photomedicine and also for studies of thermal processes in heterogeneous media, etc.

REFERENCES

1. M. Wolbarsht (Editor), *Laser Application in Medicine and Biology*. Plenum Press, New York (1974).

2. D. Sliney and M. Wolbarsht, *Safety with Lasers and Other Optical Sources. A Comprehensive Handbook*. Plenum Press, New York (1982).
3. *Extended Abstracts of the Papers Submitted to the All-Union Conference on Laser Application in Medicine*, Krasnoyarsk (1983).
4. P. V. Preobrazhenskiy, V. I. Shostak and L. I. Balashevich, *Light Impairment of the Eye*. Izd. Meditsina, Leningrad (1986).
5. T. J. White and M. A. Mainster, Chorioretinal thermal behaviour, *Bull. Math. Biophys.* **32**, 315–322 (1970).
6. G. I. Zheltov, N. G. Kondrashov, A. S. Rubanov and L. A. Linnik, Thermochemical effects during the action of laser radiation on the eyeground tissues, *Kvant. Elektronika* **6**, 1296–1303 (1979).
7. G. I. Zheltov, V. N. Glazkov, L. A. Linnik, G. G. Meshkov, A. V. Privalov and V. S. Repyakh, A thermochemical computational model for maximum permissible levels of the retina irradiation in the near IR-range, *Kvant. Elektronika* **10**, 1684–1685 (1983).
8. A. J. Welch and G. D. Polhaumus, Measurement and prediction of thermal injury in the retina of the rhesus monkey, *IEEE Trans. Biomed. Engng* **BME-31**, 633–644 (1984).
9. R. Birngruber, F. H. Hillenkamp and V.-P. Gabel, Theoretical investigations of laser thermal retinal injury, *Health Physics* **48**, 781–796 (1985).
10. J. D. Hayes and M. Wolbarsht, Thermal model for retinal damage induced by pulsed lasers, *Aerospace Medicine* **39**, 474–796 (1968).
11. W. P. Hansen and S. Fine, Melanin granule models for pulsed lasers induced retinal injury, *Appl. Opt.* **7**, 155–159 (1968).
12. D. G. Sliney, Restrictions for laser irradiations, *Kvant. Elektronika* **5**, 2271–2281 (1978).
13. D. G. Sliney, Mechanisms of interaction of laser radiation with eye tissues, *Kvant. Elektronika* **8**, 2640–2649 (1981).
14. E. P. Zege, A. P. Ivanov and I. L. Katsev, *Image Transfer in a Scattering Medium*. Izd. Nauka i Tekhnika, Minsk (1985).
15. V. K. Pustovalov and G. S. Romanov, The theory of heating and evaporation of a spherical particle exposed to optical radiation, *Int. J. Heat Mass Transfer* **28**, 277–289 (1985).
16. V. K. Pustovalov and D. S. Bobuchenko, Investigation of non-linear heat exchange of a spheroidal particle, heated by optical radiation, with the surrounding medium, *Dokl. AN BSSR* **30**, 513–516 (1986).
17. G. Arfken, *Mathematical Methods in Physics*. Atomizdat, Moscow (1970).
18. G. V. Burdzhanadze, Ye. I. Tiktopulo and P. L. Privalov, Denaturation enthalpy and entropy of collagens differing in thermal stability, *Dokl. AN SSSR* **293**, 720–724 (1987).
19. A. A. Samarsky, *The Theory of Difference Schemes*. Izd. Nauka, Moscow (1978).
20. N. N. Kalitkin, *Numerical Methods*. Izd. Nauka, Moscow (1978).
21. V. K. Pustovalov and I. A. Khorunzhii, Modelling of the process of selective interaction between optical radiation and pigmented granules in heterogeneous biotissues. In *Laser Application in Biology, Extended Abstracts of IV All-Union School-Seminar*, Kishinyov, pp. 177–182 (1986).
22. V. K. Pustovalov and I. A. Khorunzhii, Thermal processes during the interaction of optical radiation with heterogeneous laminated biotissues, *Inzh.-fiz. Zh.* **53**, 264–271 (1987).
23. N. B. Vargaftik, *Handbook of the Thermophysical Properties of Gases and Liquids*. Izd. Nauka, Moscow (1972).
24. J. D. Lund and E. S. Beatrice, Ocular hazard of short pulse argon laser irradiation, *Health Physics* **36**, 7–11 (1979).
25. R. P. Anderson and J. A. Parrish, Selective photothermolysis. Precise microsurgery by selective absorption of pulsed radiation, *Science* **220**, 524–527 (1983).
26. V. K. Pustovalov and I. A. Korunzhii, Selective interaction of laser radiation pulses with pigmented biotissues. In *Extended Abstracts of Papers Submitted to XII All-Union Conference on Coherent and Non-linear Optics*, Moscow, pp. 175–176 (1985).
27. W. S. Weinberg, R. Birngruber and B. Lorenz, The change in light reflection of the retina during therapeutic laser photocoagulation, *IEEE J. Quant. Electron.* **QE-20**, 1481–1489 (1984).
28. V. K. Pustovalov and I. A. Khorunzhii, Selective interaction of laser radiation short pulses with pigmented biotissues considering their granular structure, *Kvant. Elektronika* **13**, 1461–1466 (1986).
29. D. H. Sliney and B. C. Freasier, Evaluation of optical radiation hazards, *Appl. Opt.* **12**, 1–24 (1973).
30. P. S. Avdeyev, Yu. D. Berezin, V. V. Volkov, Yu. P. Gudakovskiy, O. V. Konovalov, P. V. Preobrazhenskiy and V. P. Muratov, The biological action of the laser infrared radiation with a wavelength of 1.06 μm on the eyeground tissue, *Vestnik Oftalmologii* No. 1, 26–30 (1982).
31. M. Born and E. Wolf, *Principles of Optics*. Pergamon Press, Oxford (1964).
32. D. V. Sivukhin, *Optics*. Izd Nauka, Moscow (1985).
33. M. B. Vinogradova, O. V. Rudenko and A. P. Sukhorukhov, *The Wave Theory*. Izd. Nauka, Moscow (1979).
34. J. A. Fleck, J. J. Morris and M. D. Feit, Time-dependent propagation of high energy laser beams through the atmosphere, *Appl. Phys.* **10**, 129–134 (1976).
35. A. J. Campillo, J. E. Pearson, S. L. Shapiro and N. J. Terrel, Fresnel diffraction effects in the design of high-power laser systems, *Appl. Phys. Lett.* **23**, 85–87 (1973).
36. B. Lachenmayr, R. Birngruber and V.-P. Gabel, The wavelength dependence of light absorption in the fundus of the eye, *Docum. Ophthalm. Proc. Ser.* **36**, 3–10 (1984).
37. R. Birngruber, V.-P. Gabel and F. Hillenkamp, Experimental studies of laser thermal retinal injury, *Health Physics* **44**, 519–531 (1983).

MECANISMES THERMIQUES PENDANT L'INTERACTION DES PULSATIONS DE RAYONNEMENT OPTIQUE AVEC DES BIOTISSUS LAMINES HETEROGENES

Résumé—On étudie théoriquement l'absorption d'énergie, le transfert thermique et les mécanismes thermochimiques pendant l'interaction des pulsations de rayonnement optique avec des granules sphériques et sphéroïdaux dans des biotissus laminés hétérogènes. Un système d'équations est formulé pour décrire les mécanismes d'interaction lors de pulsations courtes $t_p < 10^{-6}$ s et pour des pulsations longues $t_p > 10^{-6}$ s. Des solutions numériques de ce système donnent les distributions spatio-temporelles de température, les degrés des transformations thermochimiques des molécules du biotissu autour des granules pigmentés et dans le volume des biotissus laminés. On montre la possibilité de l'interaction sélective entre des pulsations radiatives courtes et les biotissus pigmentés à cause de la formation de microrégions de thermodénaturation dans et près des granules pigmentés.

THERMISCHE VORGÄNGE BEI PULSIERENDER BESTRAHLUNG VON HETEROGENEM LAMINIERTEM ZELLGEWEBE

Zusammenfassung—Strahlungsabsorption, Wärmeübergang und thermo-chemische Vorgänge, die während der pulsierenden Bestrahlung von pigmentierten kugelförmigen und ellipsoiden Körnern in heterogenem laminiertem Zellgewebe auftreten, werden theoretisch untersucht. Ein System von Gleichungen beschreibt die Vorgänge in den Körnern für kürzere ($t_p < 10^{-6}$ s) und längere ($t_p > 10^{-6}$ s) Strahlungsimpulse. Die räumliche und zeitliche Temperaturverteilung sowie der Grad der thermo-chemischen Umwandlung der Zellmoleküle rund um die pigmentierten Körner und im Bereich des laminierten Zellgewebes werden numerisch berechnet. Die Möglichkeit der gezielten Beeinflussung durch kurze Strahlungsimpulse auf pigmentierte Körner wird dadurch nachgewiesen, daß im und nahe dem pigmentierten Korn eine thermische Denaturierung auftritt.

ТЕПЛОВЫЕ ПРОЦЕССЫ ПРИ ВЗАИМОДЕЙСТВИИ ИМПУЛЬСОВ ОПТИЧЕСКОГО ИЗЛУЧЕНИЯ С ГЕТЕРОГЕННЫМИ СЛОИСТЫМИ БИОТКАНЯМИ

Аннотация—Теоретически исследованы поглощение энергии, теплообмен и термохимические процессы при взаимодействии импульсов оптического излучения с пигментированными сферическими и сфероидальными гранулами в гетерогенных слоистых биотканях. Сформулирована система уравнений, описывающая процессы взаимодействия для коротких с длительностью $t_p < 10^{-6}$с и длинных с $t_p > 10^{-6}$с импульсов излучения. На основе численного решения сформулированной системы уравнений получены пространственно-временные распределения температуры, степени термохимических превращений молекул биоткани вокруг пигментированных гранул и в объеме слоистых биотканей. Показана возможность селективного взаимодействия коротких импульсов излучения с пигментированными биотканями, заключающегося в образовании микрообластей термоденатурации внутри и вблизи пигментированных гранул.